

# Low-Pressure Burning of Catalyzed Composite Propellants

S. Krishnan\* and C. Periasamy†  
Indian Institute of Technology, Madras, India

Burning characteristics under subatmospheric pressure have been studied for uncatalyzed and catalyzed ammonium perchlorate/carboxy-terminated polybutadiene composite propellants. The catalysts used are copper chromite, copper chromate, ferric oxide, ferrocene, and ferric acetylacetonate. The studies comprise: 1) micrograph analysis with a scanning electron microscope of extinguished propellant samples at low-pressure deflagration limits (LPDL), 2) effects of catalyst concentration on LPDL, and 3) influence of catalysts on burning rate characteristics in subatmospheric as well as high pressures. The possibility of heterogeneous interfacial reactions at the fuel oxidizer boundary is demonstrated. It is shown that, when compared to iron catalysts, the catalytic effect of copper catalysts is generally less at subatmospheric pressures and greater at high pressures.

## Introduction

SEVERAL models have been proposed in the literature to explain the burning mechanism of composite solid propellants.<sup>1-5</sup> The multiple flame structure of the Beckstead-Derr-Price (BDP) model<sup>5</sup> has largely been accepted and has gone through many modifications.<sup>6,7</sup> At subatmospheric pressures, the combustion zone thickness is large and the oxidizer and fuel have enough time to mix to form a premixed flame. The characteristics of the combustion zone are expected to be same as for homogeneous propellants.<sup>8</sup> Therefore, at subatmospheric pressures, the heat feedback contribution to the burning surface is predominantly by the almost premixed and, hence, kinetics-dependent oxidizer/binder flame. Thus, a systematic experimental analysis under this limiting low-pressure subatmospheric regime for catalyzed and uncatalyzed composite propellants may lead to a better understanding of their burning mechanism.

Subatmospheric-pressure burning rate studies on composite solid propellants were done by Silla,<sup>9</sup> Steinz and Summerfield,<sup>10</sup> and Cookson and Fenn.<sup>11</sup> Silla studied ammonium perchlorate/polystyrene propellants to report that the burning rate curve did not fit Summerfield's two-third burning rate law. Steinz and Summerfield summarized the data of earlier studies on subatmospheric burning rates and then conducted further experiments on AP composite propellants with various types of fuel resins. They demonstrated that the subatmospheric burning rate data fit well with their modified GDF theory. Cookson and Fenn showed that the low-pressure deflagration limit (LPDL) is dependent on the strand size and evolved a procedure to obtain the LPDL for strands of infinite extent (adiabatic strand). No study has been reported on the exact surface structure of composite solid propellants under subatmospheric burning. The influence of catalysts on the LPDL is an important point in the study of composite propellants. The exact role played by the catalysts at the surface and in gas-phase reactions of the burning propellant has not been well understood (for example, see Ref. 12). Therefore, the present work addresses these points by the study of 1) the surface structure of extinguished ammonium perchlorate (AP) composite propellant samples at LPDL through a scanning electron microscope (SEM), 2) the effects of catalysts on LPDL, and 3) the burning rate char-

acteristics of catalyzed and uncatalyzed ammonium perchlorate/carboxy-terminated polybutadiene (AP/CTPB) propellants in subatmospheric as well as high-pressure regimes.

## Experimental Procedure

The propellant composition used for the study is given in Table 1. The AP oxidizer, CTPB binder, di-2-ethylhexyl adipate (DOA), and curing agents were provided by Vikram Sarabhai Space Center, Trivandrum, India. Dried AP powder of weight mean diameter ( $d_w = \sum n_i d_i^4 / \sum n_i d_i^3$ ) 69  $\mu\text{m}$  was used for all batches. The catalysts used were of laboratory reagent quality and their sources are also given in Table 1. Casting of the propellant was done in a vacuum ( $10^{-2}$  Torr). Each of the cured propellant blocks was checked for void content by measuring the propellant density and comparing it with the theoretical density. A less than 1% deviation in density was achieved.

The experimental setup used for the low-pressure study was similar to one used by Steinz and Summerfield,<sup>10</sup> consisting of a bell jar connected to a vacuum pump through a large surge tank. For the high-pressure experiments, a conventional strand burner with a window glass arrangement was used. The burning was carried out in a nitrogen atmosphere. In order to obtain the LPDL, the propellant strands were ignited electrically by a nichrome wire at a sufficiently high subatmospheric pressure ( $\sim 0.2$  bar) and then the pressure was slowly reduced until extinction; if the pressure was reduced too rapidly, extinction would inevitably occur at a pressure higher than LPDL. Therefore, extreme care was taken to reduce the pres-

Table 1 Propellant ingredients

Chemical	Mass fraction
AP Oxidizer	0.8000
CTPB Binder	0.1360
DOA Wetting agent	0.0453
MAPO Curing agent	0.0124
GY252 Curing agent	0.0062
Catalyst replaces the equivalent mass of oxidizer	
Catalyst	Source
Copper chromite ( $\text{CuCr}_2\text{O}_4$ )	PL Industry, India
Copper chromate ( $\text{CuCrO}_4$ )	Burgoyre, India
Ferric oxide ( $\text{Fe}_2\text{O}_3$ )	Sarabhai M Chemicals, India
Ferrocene ( $\text{C}_{10}\text{H}_{10}\text{Fe}$ )	Fluka, Switzerland
Ferric acetylacetonate [ $\text{Fe}(\text{C}_5\text{H}_7\text{O}_2)_3$ ]	Fluka, Switzerland

Received March 11, 1985; revision received Feb. 21, 1986. Copyright © American Institute of Aeronautics and Astronautics, Inc., 1986. All rights reserved.

\*Associate Professor, Department of Aeronautical Engineering.

†Project Associate, Department of Aeronautical Engineering.

sure as slowly as possible. The extinguished samples were prepared for SEM (Cambridge Stereoscan S-180, Cambridge Instrument Co. Ltd., England) microphotography with a vacuum deposition of approximately 100 Å of gold. In order to find the burning rates of the propellant in both the subatmospheric- and high-pressure regimes, the time to burn a known length of propellant strand was measured by an electronic timer; the melting of two fuse wires introduced in the strand at known distances was used to create necessary signals in a suitable relay circuitry to start and stop the timer. Every burning rate test was repeated at least once to check the consistency of the data. The repeatability of burning rate data was better for the high-pressure range (HPR), 5-65 bars, than for subatmospheric-pressure range (SPR). Only burning rate values obtained within a 3% variation were considered acceptable. Batch-to-batch consistency was also checked by casting a few compositions twice. All of the burning rate data were fitted separately for SPR and HPR with the burning rate equation  $r = ap^n$  by the method of least squares fit. The standard deviation of the fit was always less than 0.04. A typical plot in the SPR is shown in Fig. 1.

## Results and Discussion

### Visual Observation of Subatmospheric Flame

The flame was observed visually through the bell jar glass wall at a distance of about 15 cm from the burning propellant surface. The burning could be observed in a completely dark environment with or without a magnifying lens (magnification ~2.5; however, the dimensions specified here are without magnification). The flame was generally of two stages: a base flame sitting on the surface (transparent blue for copper-salt catalyzed propellants and less luminescent light orange for iron-salt catalyzed and uncatalyzed propellants), followed by a top flame (blue and orange mixed for copper-salt catalyzed propellants and yellow-to-orange for iron-salt catalyzed and uncatalyzed propellants). On the visible burning surface, bright deep-orange flamelets  $\frac{1}{2}$  mm or less in diameter and lasting about  $\frac{1}{4}$  s emerged. The flamelets were either very close ( $\frac{1}{2}$  mm or less) and interconnected or far apart (~2 mm). Although these flamelets were seen in both catalyzed and uncatalyzed propellants, it appeared qualitatively that these flamelets are more in number for catalyzed propellants.

At sufficiently high-subatmospheric pressure (0.6-0.7 bar), the total flame height was several centimeters long (7-10 cm), the base flame being about 1 mm high. Bright light-orange streaks were frequently seen over the entire length of the flame. As the pressure was lowered (0.2-0.3 bar), the top flame became shorter (~2 cm) and more uniform (with no visible bright streaks). White fumes emanated from the burning surface and were deposited on the relatively cooler surfaces of the apparatus. As the pressure was further lowered near the LPDL: 1) the top flame became almost transparent with little height (~1 cm); 2) the base flame became inflated (2-3 mm); 3) for uncatalyzed and iron-salt catalyzed propellants, a thin blue layer of flame appeared between the propellant surface and the less luminescent light-orange base flame; 4) the fuming intensity increased; 5) relatively large reacting particles were ejected from the burning surface, passing through the flame and falling to the bottom of the apparatus; and 6) bright deep-orange flamelets continued to emerge on the burning surface. With the very slow rate of decrease in the pressure, the extinction crept in from the edges of strand. From the start of extinction, the patch of the burning area with the bright deep-orange flamelets kept shrinking and the overall reaction patch kept shifting from place to place. The LPDL was taken as the pressure at which complete extinction occurred. The extinguished surface was relatively deep around the center, indicating that the last extinction occurred there.

The fume deposit on the bell jar wall and the relatively large particles ejected from the burning surface under low-subatmospheric burning were subjected to further investiga-

tion. A beaker with a wide mouth was kept below the burning strand within the bell jar setup to collect the ejected particles. The infrared spectrum of the particles thus collected revealed that they were of AP. Also, through SEM micrographs, the ejected particles collected on glass plates were found to be similar to the partially reacted AP crystals seen on the surface of the extinguished samples, see Fig. 2. The i.r. spectra of the fume deposits of different propellants were similar and indicated the presence of ammonium chloride (AC) and AP. After comparing the spectra of standard mixtures of AC and AP, the fume deposits were estimated to contain AC and AP in a ratio of about 90:10 by weight. A chemical analysis was also made of the fume deposit of the uncatalyzed propellant. A measured quantity of deposit was dissolved in distilled water and filtered. A black residue, possibly carbon and/or partially reacted pyrolyzed resin, was obtained. A known quantity of filtrate was reacted with a known quantity of sodium hydroxide and boiled to remove the ammonia. The unreacted sodium hydroxide was found by titrating with standard hydrochloric acid and the weight contents of AC and AP were calculated. This total weight of AC and AP was compared with the residue obtained from the known volume of filtrate through vacuum drying. The mass balance was achieved within the error limits specified. The total chemical analysis revealed by weight percentage was: black residue  $6.7 \pm 0.8\%$ ,  $\text{NH}_4\text{Cl}$   $82.6 \pm 1.5\%$ , and  $\text{NH}_4\text{ClO}_4$   $10.7 \pm 1.5\%$ .

In the earlier flame observations (all visual) under low subatmospheric pressures, other investigators have reported the disappearance of the bright streaks at high subatmospheric pressure, with the flame becoming more uniform and shorter,<sup>9</sup>

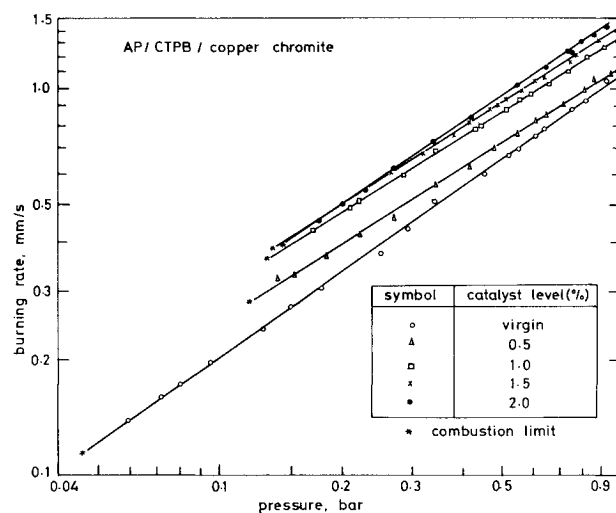


Fig. 1 Effect of copper chromite on propellant burning at subatmospheric pressure.

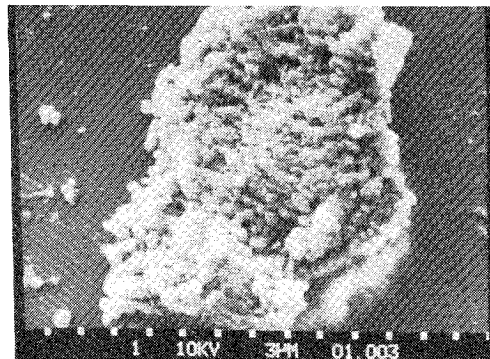
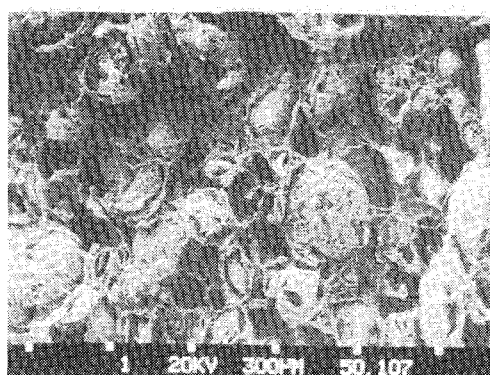
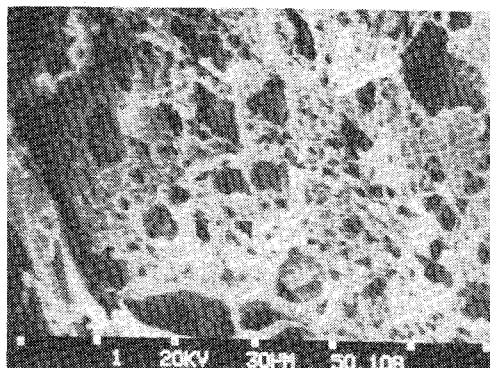


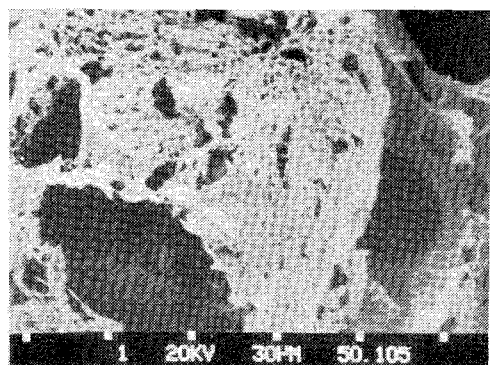
Fig. 2 SEM micrograph of a partially reacted AP particle ejected from the subatmospheric pressure burning surface of an uncatalyzed AP/CTPB propellant.



a) Overall view.



b) Thin layer with pores covering partially reacted AP particle.



c) Hollow shell.

Fig. 3 SEM micrographs of extinguished sample at LPDL of 1.0% ferric oxide catalyzed AP/CTPB propellant.

and the white fuming and ejection of particles.<sup>10</sup> The identification of bright deep-orange flamelets on the burning surface is the new element in our observation. The dark zone above the burning propellant surface (3-5 mm thick at extinction), as reported by Steinz and Summerfield,<sup>10</sup> is not present in our case, except for a thin blue layer appearing near the extinction of uncatalyzed and iron-salt catalyzed propellants (in the copper-salt catalyzed propellants there are no means available to distinguish this third stage of flame development since the corresponding base flame is already blue); Steinz and Summerfield used finer AP particles (5  $\mu\text{m}$ ) and more fuel-rich propellants (AP = 65-75%).

#### SEM Micrographs

SEM micrographs were made of all the extinguished samples at LPDLs, a few of which are shown in Figs. 3-7. Since the pictures all represent surfaces (uncatalyzed and catalyzed) at extinction, they appear to be essentially the same, characterized by complicated three-dimensional surface structures with potholes and burrows (Fig. 3a), partially decomposed AP

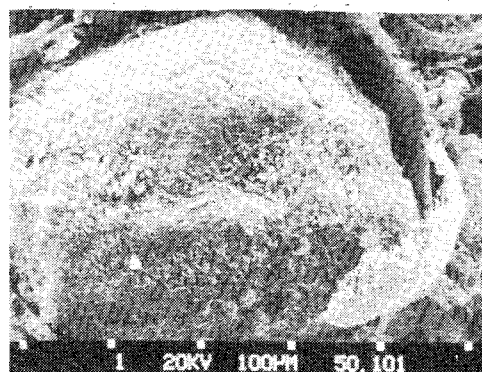


Fig. 4 SEM micrograph of extinguished sample at LPDL of 1.5% ferric oxide catalyzed AP/CTPB propellant.

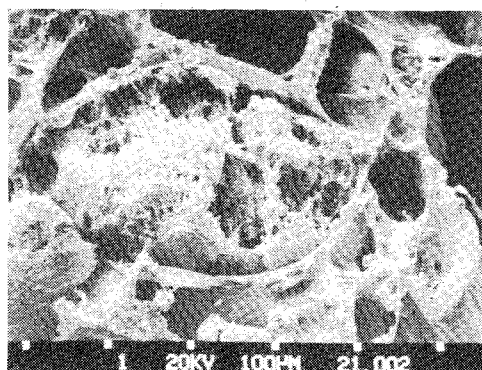


Fig. 5 SEM micrograph of extinguished sample at LPDL of uncatalyzed AP/CTPB propellant showing thick spongy layer covering partially decomposed AP particle.

particles (Figs. 3a and 4-7), recesses at the AP/binder interfaces (Figs. 3a and 4-7), and continuous binder wall matrices with frothy top layers (Figs. 3a, 4, 5, and 7). The partially decomposed AP particles exhibit three distinct stages: 1) a near-surface structure, but with slight porosity (Fig. 4); 2) a porous flaky structure, many times partially or fully covered by a layer, either thick ( $\sim 5 \mu\text{m}$ ) and spongy (Fig. 5) or thin ( $\sim 1 \mu\text{m}$ ) with pores of various sizes and shapes (Figs. 3b, 6, and 7); and 3) a hollow shell with wall pores ( $> 1 \mu\text{m}$ ) of various sizes and shapes and usually with one or two large vent-out holes (Figs. 3a and 3c). The fact that the layer, when present (stage 2), was not part of the porous structure beneath was confirmed in our SEM views of samples having insufficient gold-coating (unintentional) when the layer started drifting (due to the charging effect of the electron beam) independent of the porous structure beneath. The extinguished samples were vertically sliced and then viewed through the SEM; the burrows were seen to extend to about two to three mean particle diameters. In order to check whether the surface structure of the slowly extinguished sample at LPDL was similar to that of the rapidly extinguished sample above LPDL, a few propellant samples burning sufficiently above LPDL ( $\sim 0.2$  bar) were rapidly extinguished. The corresponding SEM micrographs showed surface structures similar to those of the slowly extinguished samples at LPDL.

In the high-pressure burning regime, the presence of a melt layer over the surface of AP particle has been reported by many studies.<sup>13-16</sup> In the subatmospheric-pressure regime (SPR), the partially decomposed AP particles seen in our SEM micrographs show a porosity very similar to particles that experienced partial slow decomposition in the controlled heating experiments made by Boggs and Kraeutle.<sup>17</sup> The thick spongy layer (or the thin layer with pores) over the partially gasified AP particle and the hollow shell with wall pores seen

Table 2 Comparison of catalytic effectiveness at 0.5 and 30 bars

Catalyst	Concentration, %	Z	
		Low pressure, 0.5 bar	High pressure, 30 bar
CuCr <sub>2</sub> O <sub>4</sub>	0.5	1.080	1.437
	1.0	1.311	1.641
	1.5	1.375	1.714
	2.0	1.416	1.745
CuCrO <sub>4</sub>	0.5	1.150	1.374
	1.0	1.252	1.529
	1.5	1.231	1.553
	2.0	1.355	1.627
Fe <sub>2</sub> O <sub>3</sub>	0.5	1.355	1.365
	1.0	1.449	1.456
	1.5	1.509	1.553
	2.0	1.547	1.564
C <sub>10</sub> H <sub>10</sub> Fe	0.5	1.051	1.223
	1.0	1.259	1.277
	1.5	1.327	1.488
	2.0	1.419	1.499
Fe(C <sub>5</sub> H <sub>7</sub> O <sub>2</sub> ) <sub>3</sub>	0.5	1.040	1.329
	1.0	1.269	1.398
	1.5	1.379	1.506
	2.0	1.425	1.595

in our micrographs appear to have been formed because of the recondensation of the gasified AP vapor. We could not quantify the conditions under which the thick spongy layer or the thin layer is present. However, the thick spongy layer, when present, is usually in the uncatalyzed propellants.

The most revealing characteristic of the subatmospheric burning surface is the presence of a recess at the AP/binder interface in both the catalyzed and uncatalyzed propellants. This recess, termed the "undercutting" or "undermining" of the AP particle, was observed at pressures below 20.7 bar (300 psi) by Boggs et al.<sup>14</sup> and Derr and Boggs<sup>15</sup> in their SEM studies for fuel-rich (22-26%) AP/PU propellants. There are no reports of recesses at the AP/binder interfaces of typical composite propellants at rocket motor pressures. However, in the pressure range of 140-10 bars for uncatalyzed AP/polymer sandwiches with thin polymer films of thicknesses normally found in composite propellants, Price et al.<sup>18</sup> reported that the binder film became recessed below the surface and that *this recess was conspicuous at lower pressures (~10 bars)*. Thus, it can be seen that, although there are no reports of recesses at the AP/binder interface in typical composite propellants at rocket motor pressures, there is experimental evidence of the recess in the low-pressure range.

In the low-pressure propellant burning range (below the AP deflagration limit), the gas-phase reactions are expected to be caused mainly by the AP/binder flame whose leading edge ("phalanx" kernel base) is the premixed flame.<sup>18,19</sup> The extent of this premixed flame reaction increases with further decreases in pressure. In the SPR, the gas-phase reactions may be entirely dominated by this transparent, slightly luminous, inflated, and blunt "phalanx" kernel base; this transparent and slightly luminous flame condition has been observed in the present study as well as those reported in Refs. 9 and 10. At this juncture, the following question arises: while the propellant burning surface appears to be covered by the premixed flame, what are those bright deep-orange flamelets seen on the burning surface? According to Powling,<sup>20</sup> in the low-temperature decomposition of AP (<300°C) a solid-phase exothermic decomposition (to Cl<sub>2</sub>, O<sub>2</sub>, H<sub>2</sub>O, and N<sub>2</sub>O) can accompany the sublimation (to NH<sub>3</sub> and HClO<sub>4</sub>) under certain flame conditions to become a major source of the energy release on or near the surface; the reactive products of this exothermic solid-phase decomposition (Cl<sub>2</sub> or O<sub>2</sub>) can

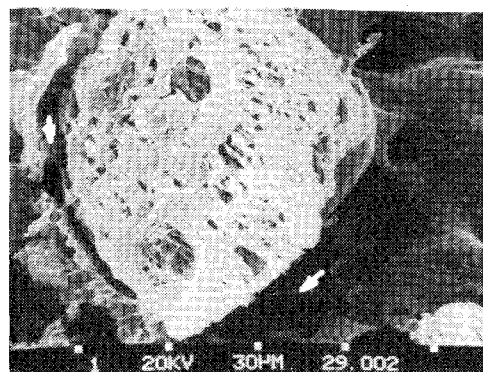


Fig. 6 SEM micrograph of extinguished sample at LPDL of 0.5% ferric acetylacetonate catalyzed AP/CTPB propellant.

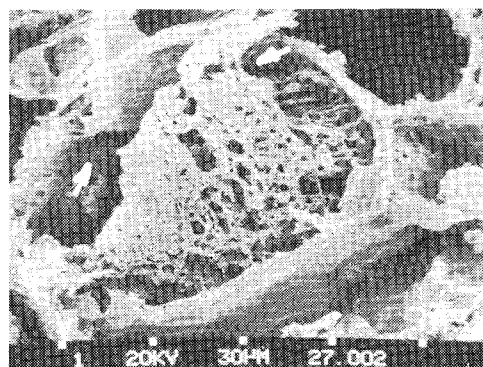


Fig. 7 SEM micrograph of extinguished sample at LPDL of 2% ferric oxide catalyzed AP/CTPB propellant.

combine with adjacent fuel elements before the onset of homogeneous gas-phase reactions with NH<sub>3</sub>, HClO<sub>4</sub>, and fuel gases. In his theory of composite propellant burning, Hermance proposed that an intense heterogeneous interfacial reaction caused the formation of fissures at the AP/binder interface and demonstrated good agreement between theoretical and experimental burning rates over a wide range of pressures.<sup>4</sup> In view of this, it is possible that the visually observed deep-orange flamelets represent intense interfacial heterogeneous reactions. The recesses in our SEM micrographs, as well as in the micrographs of Refs. 14 and 15, may be taken as the intense interfacial reaction zones. Considering the visual estimate of the flamelet characteristics detailed in the previous section and the SEM micrographs of the extinguished surfaces, the flamelets possibly represent the intense interfacial reaction zones around large AP particles 200 μm or more in diameter. The extent to which this heterogeneous reaction might occur in the total combustion remains difficult to predict. However, it is likely that, as the pressure increases, the gas-phase processes may become more pressure dependent at a faster pace than the heterogeneous combustion processes.<sup>21</sup>

In view of the above, it seems to us that, due to three-dimensional heating (heat from the interfacial reaction as well as from the phalanx kernel), the partially gasified AP particles are either prematurely released due to undercutting (more likely for larger particles) or completely gasified (more likely for smaller particles), resulting in the formation of potholes. See Figs. 3a, 5, and 7. In such potholes, if fresh AP particles are exposed, further intense reaction at the new AP boundary possibly starts well below the top layer and results in burrows. See Figs. 3a, 3c, and 5.

#### Effects of Catalysts

Figure 8 shows the variation of the LPDL with the weight percentage of the catalysts. In all catalysts, LPDL is found to

increase with the catalyst concentration. We find that the LPDL increases at a faster pace with copper catalysts than with iron catalysts. Values of the catalytic effectiveness  $Z$ , defined as the ratio of the burning rates of catalyzed and uncatalyzed propellants at the same pressure, are presented in Table 2. Generally, the value of  $Z$  increases with the catalyst concentration and pressure. However, in the case of  $\text{Fe}_2\text{O}_3$ , the variation of  $Z$  from SPR to HPR is the smallest. In SPR, it is seen that  $\text{Fe}_2\text{O}_3$  has the highest  $Z$  of all the catalysts; the  $Z$  of  $\text{CuCr}_2\text{O}_4$ , the best burning rate enhancer in the HPR, is second to that of  $\text{Fe}_2\text{O}_3$ . It is noted from the overall results of catalytic effectiveness that copper catalysts have a higher catalytic effect with the increase in pressure than iron catalysts. Also, plotting LPDL vs  $Z$  for the catalysts considered suggests a possible correlation between them. In the SPR, as the catalyst concentration is increased, the  $n$  value generally

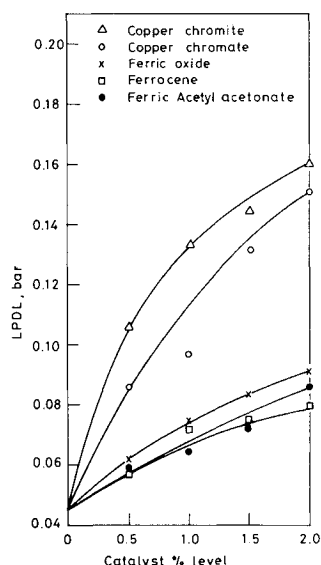


Fig. 8 Variation of LPDLs with catalyst concentration.

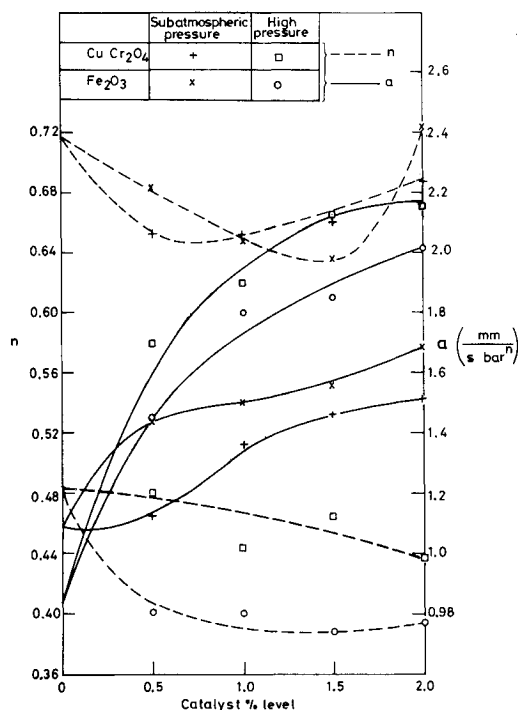


Fig. 9 Variation of  $n$  and  $a$  values in subatmospheric- and high-pressure ranges.

first decreases and then increases, demonstrating a conspicuous minimum value; in the HPR, as the catalyst concentration is increased, the  $n$  value decreases. See Fig. 9. As evidenced by the catalytic effectiveness shown in Table 2, the catalysts can alter the reactions either on the surface or in the gas phase, or both. We may attribute the increase in the LPDL with the catalyst concentration to the increased interfacial heterogeneous reactions, which result in faster undercutting around the AP particles and hence their premature release from the surface. Thus, the extinction may be due to oxidizer depletion at the burning surface combined with low-pressure combustion inefficiency. Investigating this point, we tried to compare the appearance of the extinguished samples with and without catalysts. Due to the highly complicated three-dimensional surface structure, we could not estimate the differences in the extent of recess formation. However, as mentioned earlier, under visual observation, the bright deep-orange flamelets appear qualitatively more in number (possibly due to the higher intensity of interfacial reactions) for catalyzed propellants.

In view of the various studies on composite propellant catalysts,<sup>20-24</sup> it appears reasonable to consider two groups of catalysts for the convenience of discussion: 1) catalysts that augment primarily the gas-phase reaction rate and secondarily the surface reaction rate, and 2) catalysts of functions opposite to those of group 1. While the catalysts of first group (enhancing primarily the temperature gradient in the gas-phase reaction zone) make  $Z$  more sensitive in the HPR, the catalysts of second group make  $Z$  less sensitive in the HPR and possibly provide more heat at the surface (even at lower pressure). If a catalyst were to augment the surface reaction rates, catalysis at high pressures should be no more pronounced than at atmospheric or lower pressures since the extent of the high-temperature penetration into the surface and, hence, the residence time allotted for catalytic reactions beneath the surface sharply decrease as the burning pressure increases.<sup>22</sup>

In the present study, by the addition of catalysts, it is the intensity of the construed interfacial heterogeneous reactions under low pressures that seem to be augmented, as demonstrated by the LPDL variation. The increased interfacial reactions, a common feature of both the groups (although not of equal strength), can under low pressure cause more complete gasification of the AP at the surface, thus increasing the burning rate; and, due to faster undercutting and the consequent premature ejection of the AP particles, at the limit cause a paucity of AP at a higher LPDL. Thus, when compared to the first group, the second group of catalysts has the capacity of providing more heat at the surface even at lower pressures (higher burning rate) and, due to greater gasification of the AP particle at the surface, delay the imminent rise in the LPDL (lower rise in LPDL). Thus,  $\text{Fe}_2\text{O}_3$  probably belongs more closely to the second group of catalysts.

## Conclusions

1) The possible presence of interfacial heterogeneous reactions on composite solid propellant burning surfaces is demonstrated. The "blunt," premixed leading edge of the low-pressure AP/binder flame cannot sharply "undercut" the oxidizer boundary. The bright deep-orange flamelets seen emerging on the subatmospheric-pressure burning surface covered by the transparent and slightly luminous AP/binder premixed flame and the sharp undercutting around the oxidizer boundaries in the SEM micrographs form the supporting evidence.

2) As the catalyst's concentration increases, the low-pressure deflagration limit also increases. This is possibly due to the increased interfacial reactions that may result in faster undercutting of the AP particles and prematurely releasing the AP particles from the surface.

3) The catalytic effect of copper catalysts is generally less than that of iron catalysts at subatmospheric pressures and greater at high pressures.

### Acknowledgments

The present work forms a part of the research sponsored by the Aeronautics Research and Development Board, Ministry of Defence, India, under Sanction AERO/RD-134/100/10/81-82/303. The financial support of this research by the ARDB is gratefully acknowledged. The SEM micrographs were taken at the Regional Sophisticated Instruments Centre of IIT, Madras, India.

### References

- <sup>1</sup>Summerfield, M. et al., "Burning Mechanism of Ammonium Perchlorate Propellants," *AIAA Progress in Astronautics and Aeronautics: Solid Propellant Rocket Research*, Vol. 1, edited by M. Summerfield, Academic Press, New York, 1960, pp. 141-182.
- <sup>2</sup>Chaicken, R.F. and Andersen, W.H., "The Role of Binder in Composite Propellant Combustion," *AIAA Progress in Astronautics and Aeronautics: Solid Propellant Rocket Research*, Vol. 1, edited by M. Summerfield, Academic Press, New York, 1960, pp. 227-249.
- <sup>3</sup>Nachbar, W., "A Theoretical Study of the Burning of a Solid Propellant Sandwich," *AIAA Progress in Astronautics and Aeronautics: Solid Propellant Rocket Research*, Vol. 1, edited by M. Summerfield, Academic Press, New York, 1960, pp. 207-226.
- <sup>4</sup>Hermance, C.E., "A Model of Composite Propellant Combustion Including Surface Heterogeneity and Heat Generation," *AIAA Journal*, Vol. 4, Sept. 1966, pp. 1629-1637.
- <sup>5</sup>Beckstead, M.W., Derr, R.L., and Price, C.F., "A Model of Composite Solid Propellant Combustion Based on Multiple Flames," *AIAA Journal*, Vol. 8, Dec. 1970, pp. 2200-2207.
- <sup>6</sup>Cohen, N.S., "Review of Composite Propellant Burn Rate Modeling," *AIAA Journal*, Vol. 18, March 1980, pp. 277-293.
- <sup>7</sup>Beckstead, M.W., "A Model for Solid Propellant Combustion," *Eighteenth Symposium (International) on Combustion*, The Combustion Institute, Pittsburgh, PA, 1981, pp. 175-183.
- <sup>8</sup>Williams, F.A., Barrère, M., and Huang, N.C., "Fundamental Aspects of Solid Propellant Rockets," AGARDograph 116, 1969, p. 318.
- <sup>9</sup>Silla, H., "Burning Rates of Composite Solid Propellants at Subatmospheric Pressure," *ARS Journal*, Vol. 31, 1961, pp. 1277-1278.
- <sup>10</sup>Steinz, J.A. and Summerfield, M., "Low Pressure Burning of Composite Solid Propellants," *Propellants Manufacture, Hazards and Testing, Advances in Chemistry Series*, No. 88, American Chemical Society, Washington, DC, 1969, pp. 244-295.
- <sup>11</sup>Cookson, R.A. and Fenn, J.B., "Strand Size and Low-Pressure Deflagration Limit in a Composite Propellant," *AIAA Journal*, Vol. 8, May 1970, pp. 864-866.
- <sup>12</sup>Kishore, K. and Sunitha, M.R., "Effect of Transition Metal Oxide on Decomposition and Deflagration of Composite Solid Propellant Systems: A Survey," *AIAA Journal*, Vol. 17, Oct. 1979, pp. 1118-1125.
- <sup>13</sup>Hightower, J.D. and Price, E.W., "Experimental Studies Relating to the Combustion Mechanism of Composite Propellants," *Astronautica Acta*, Vol. 14, No. 1, 1968, pp. 11-21.
- <sup>14</sup>Boggs, T.L., Derr, R.L., and Beckstead, M.W., "Surface Structure of Ammonium Perchlorate Composite Propellants," *AIAA Journal*, Vol. 8, Feb. 1970, pp. 370-372.
- <sup>15</sup>Derr, R.L. and Boggs, T.L., "Role of Scanning Electron Microscopy in the Study of Solid Propellant Combustion, Part III: The Surface Structure and Profile Characteristics of Burning Composite Solid Propellants," *Combustion Science and Technology*, Vol. 1, 1970, pp. 369-384.
- <sup>16</sup>Boggs, T.L., Price, E.W., and Zurn, D.E., "The Deflagration of Pure and Isomorphously Doped Ammonium Perchlorate," *Thirteenth Symposium (International) on Combustion*, The Combustion Institute, Pittsburgh, PA, 1971, pp. 995-1008.
- <sup>17</sup>Boggs, T.L. and Kraeutle, K.J., "Role of Scanning Electron Microscope in the Study of Solid Rocket Propellant Combustion: 1. Ammonium Perchlorate Decomposition and Deflagration," *Combustion Science and Technology*, Vol. 1, 1969, pp. 75-93.
- <sup>18</sup>Price, E.W., Handley, J.C., Panyam, R.R., Sigman, R.K., and Ghosh, A., "Combustion of Ammonium Perchlorate-Polymer Sandwiches," *AIAA Journal*, Vol. 19, March 1981, pp. 380-386.
- <sup>19</sup>Fenn, J.B., "A Phalanx Flame Model for the Combustion of Composite Solid Propellants," *Combustion and Flame*, Vol. 12, June 1968, pp. 201-216.
- <sup>20</sup>Powling, J., "Experiments Relating to the Combustion of Ammonium Perchlorate-Based Propellants," *Eleventh Symposium (International) on Combustion*, The Combustion Institute, Pittsburgh, PA, 1967, pp. 447-456.
- <sup>21</sup>Jones, H.E. and Strahle, W.C., "Effects of Copper Chromite and Iron Oxide Catalysts on AP/CTPB Sandwiches," *Fourteenth Symposium (International) on Combustion*, The Combustion Institute, Pittsburgh, PA, 1973, pp. 1287-1295.
- <sup>22</sup>Pittman, C.U., "Location of Action of Burning Rate Catalysts in Composite Propellant Combustion," *AIAA Journal*, Vol. 7, Feb. 1969, pp. 328-333.
- <sup>23</sup>Pearson, G.S., "Composite Propellant Catalysts: Copper Chromate and Chromite," *Combustion and Flame*, Vol. 14, 1970, pp. 73-83.
- <sup>24</sup>Inami, S.H., et al., "Solid Propellant Kinetics I: The Ammonium Perchlorate-Copper Chromite-Fuel System," *Combustion and Flame*, Vol. 17, 1971, pp. 189-196.